Fabrication, Analysis and Testing of Smart Adaptive Composite Beams

Basavaraj Noolvi[a], Shanmukha Nagaraj[b] and S. Raja[c]

[a]*Dept. of Mech., Engg., Amrita School of Engg., Amrita Vishwa Vidyapeetham, Bengaluru, India*
Corresponding Author, Email: n_braj@blr.amrita.edu
[b]*Dept. of Mech. Engg., R V College of Engg., Bengaluru, India*
[c]*National Aerospace Laboratories, Bengaluru, India*

ABSTRACT:

The presented research involves two types of Smart adaptive composite beams (SAC). The study was conducted on smart composite beams composed of LY5210 and EPOLAM 2063 resin systems respectively. The fabrication of composite beams involved embedding SMA wires in between layers of 0/90 woven glass fibre in the respective resin systems, followed by suitable curing and post curing cycles. Suitable mould was designed and manufactured to facilitate the required pre-straining of SMA wires. Both static and dynamic tests were done on the SAC specimens to study the behaviour of these SACs. Static and free vibration analyses were carried out using MSC Nastran and Hypermesh. There has been good agreement between the results of finite element analysis and the experimental results.

1. Introduction

SMA composites have proven their potential applications in various areas including the control of external shape and stiffness, damage tolerance, vibration control. Different studies of the possible use of SMA composites integrated within structural elements have been developed by several researchers and published in the literature. These researches are mainly related to the following specific topics: vibration control, buckling and post buckling effects, shape control, and micromechanics of the SMA composite material [1]. It can be emphasized that the mechanical response of these composites depends upon several different factors, e.g., the curing technique followed, the pre-strain, volume fraction of the constituent elements, the selected material properties etc. Birman et al [2] worked on restrained SMA fibres embedded within plates and found to reduce the stresses and the deflection of laminates. Mathematical modelling of SMA composite constitutive law for effective properties was first attempted by Stalmans et al [3].

Marfia et al [4] studied the super elasticity and Shape Memory phenomenon for laminated SMA beams. Marfia et al [5] established a micromechanical-based modelling of the constitutive behavior of the SMA composites, characterized by an elastic matrix. Suitable homogenization rules were developed for the overall behaviour of long-fibre SMA composites. A quantitative analysis of the role of constituent properties and microstructure in the overall behavior of a SMA composite with ductile matrix based on micromechanics was carried out by Cherkaoui [6]. Chetan and Raja [7] undertook the homogenization and study of pseudo-

elastic behaviour of SMA wire reinforced composite materials. Chetan, Raja, and Upadhya have presented an exhaustive work on Micro-mechanical behaviours of same composite under hygro-thermal-elastic strain fields [8]. Lee et al [9] conducted numerical analyses of the thermal buckling behavior of composite shell laminates with SMA wires.

Basavaraj et al [10] investigated the static and dynamic properties of SMA composite beam with LY5210 resin system. This paper presents comparative study of the static and dynamic characteristics of two Smart Adaptive Composites, made of LY5210 and EPOLAM 2063 resin systems, abbreviated as SAC-1 and SAC-2 respectively. SAC specimens are fabricated by vacuum bagging method. Static and dynamic bending tests are conducted on both these specimens. Finite element analysis is carried out to obtain numerical results for static and dynamic conditions, for the same beam models. Comparative study of FEA and experimental results is presented.

2. Fabrication of SAC specimens

2.1. SAC-1 - Glass fabric-ly5210 resin SAC

SAC-1 specimens are fabricated using two SMA wires of diameter 0.38mm, between five layers of glass fabric, woven in two directions (0/90) of thickness 0.18mm, with three layers on top and two at the bottom. K-24 hardener and DY219 accelerator are used along with resin. The resin, hardener and accelerator were mixed in the ratio 100:56:1 by weight. After 3 hours of setting time in vacuum chamber, the specimens are maintained at room temperature for next 24 hours. The following post curing is performed for the specimens inside an

oven. Specimen edges of are trimmed after post curing and Fig. 1 shows the final fabricated specimen.

Table 1: Post curing cycle for SAC-1 specimen

Step	Temperature (°C)	Time (hrs.)
1	60	1
2	92	1
3	120	1
4	150	1
5	180	2

Fig. 1: SAC-1: glass fabric-LY5210 resin

2.2. SAC-2 - Glass fabric- Epolam 2063 resin SAC

Being a high temperature resin system, EPOLAM 2063 has a Tg of 190°C. Seven layers of same glass fabric of thickness 0.18mm woven in two directions, with three on top of SMA wires and four layers at the bottom are used. The same 0.38mm diameter SMA wire with 4% induced pre-strain is employed. After 6 hours of setting time in vacuum chamber, the specimen is maintained for 24 hours at room temperature, and then post curing is carried out at elevated temperatures as per the curing cycle given in the Table 2. After curing the specimen is released from the mould and the edges are trimmed. The SAC-2 specimen is shown in Fig. 2.

Table 2: Post curing cycle for SAC-2 specimen

| Step	Temperature (°C)	Time (hrs.)
1	80	6
2	180	4

**Fig. 2: SAC-2: glass fabric-EPOLAM 2063 resin**

3. Finite element analysis

In the presented both static and dynamic analysis are carried out using MSC Nastran. The FEA model is generated using Hypermesh
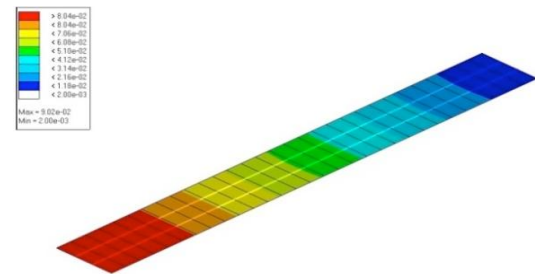
3.1. Static analysis

The glass fibre reinforced plastic (GFRP) layers of the specimens are modelled using four nodded two dimensional plate elements CQUAD4. The thickness of these elements is defined through PSHELL card. The SMA wire is modelled using 1-D beam element CBEAM. The cross sectional properties of this beam are defined using PBEAM card, which defines the area of cross section, moment of inertia. One edge of the beam is clamped using Single Point constraint (SPC) command. All the six Degrees of Freedoms (DOFs) i.e., three rotational and three linear DOF's are arrested. At the free end, a load of 1N is applied. The FEA models are shown in Fig. 3(a) and Fig. 3(b). Figs. 4 and 5 show the fringe plots of the displacement and Von-Mises stress for the above analysis. The numerical results are given in Table 3.
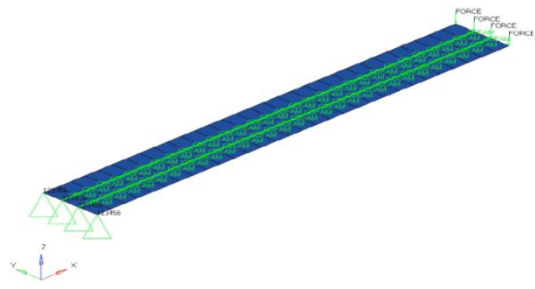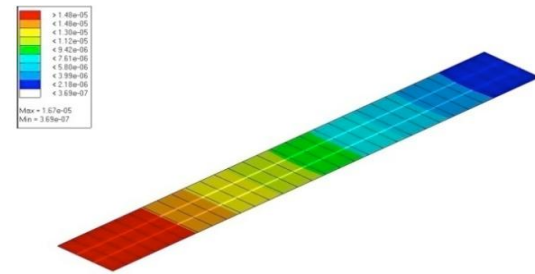

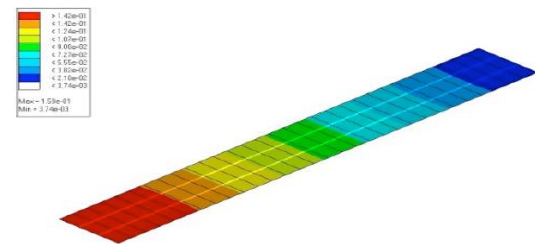**Fig. 3(a): FEA model SAC-1**
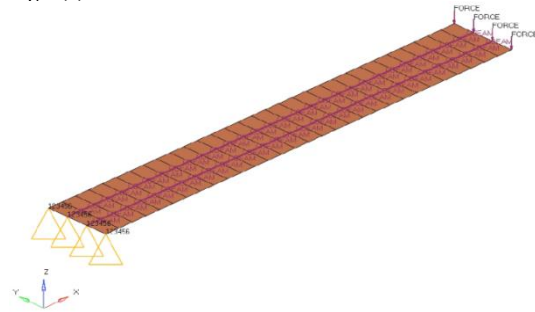
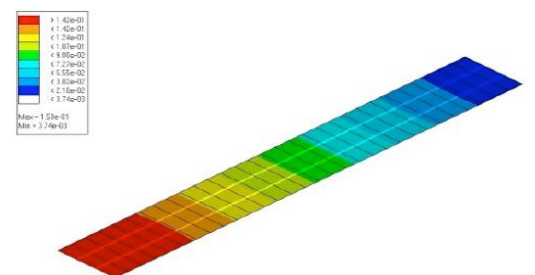**Fig. 3(b): FEA model SAC-2**

Fig. 4(a): SAC-1: Displacement

Fig. 4(b): SAC-2: Displacement


Fig. 5(a): SAC-1: Von-Mises Stress

Fig. 5(b): SAC-2: Von-Mises Stress
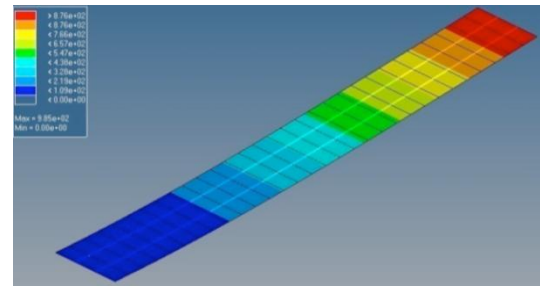
Table 3: Results of the static analysis

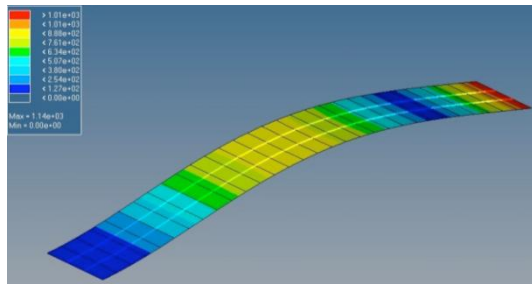| Parameter	SAC-1	SAC-2
Displacement (mm)	16.6	5.62
Von mises stress (N/mm^2)	0.09	0.159
Von mises strain (με)	16.7	0.2

3.2. Dynamic analysis

Free vibration analysis is carried out for the beam. The first five mode shapes of SAC beams are given in Fig. 6. Respective natural frequencies are given in Table 4.
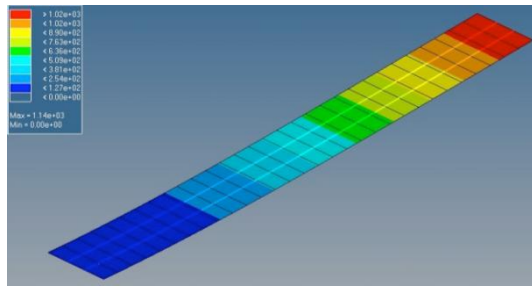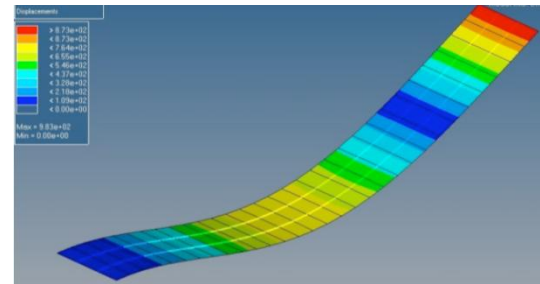

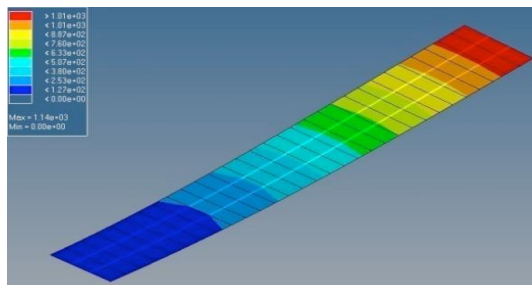**SAC-1: Mode-1 (1st transverse bending)**

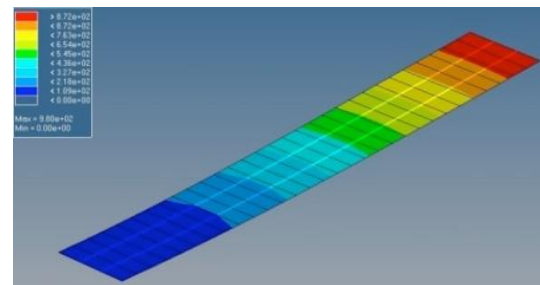**SAC-2: Mode-1 (1st transverse bending)**

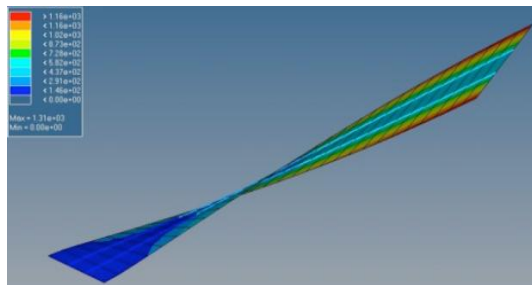**SAC-1, Mode-2 (transverse bending)**

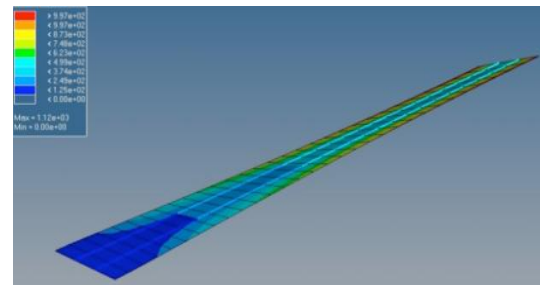**SAC-2: Mode-2 (transverse bending)**

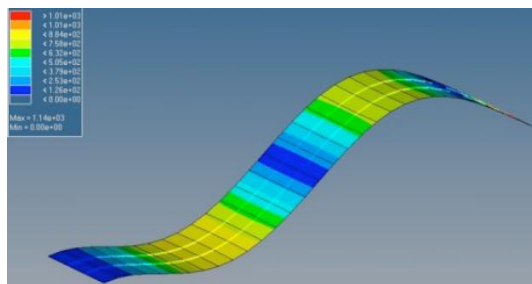**SAC-1, Mode-3 (1st lateral bending)**

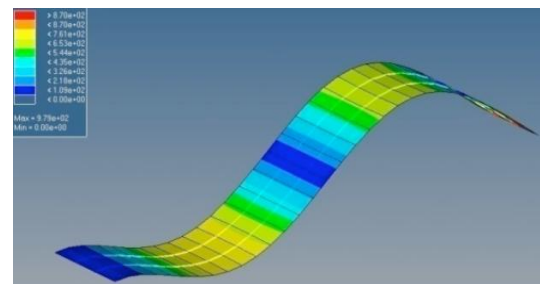**SAC-2: Mode-3 (1st lateral bending)**

SAC-1: Mode-4 (torsion mode)

SAC-2: Mode-4 (torsion mode)

SAC-1: Mode-5 (3rd transverse bending)

SAC-2: Mode-5 (3rd transverse bending)

Fig. 6: First five mode shapes of SAC beams

**Table 4: Natural frequencies for the first 5 modes**

Mode No.	Frequency (Hz) SAC-1	Frequency (Hz) SAC-2	Mode description
1	51.01	100.30	Transverse bending - 01
2	319.16	627.17	Transverse bending - 02
3	581.73	790.18	Lateral bending - 01
4	728.15	1344.29	Torsion
5	892.59	1752.36	Transverse bending

4. Experimental studies

The experimental studies of this project work involve the static and dynamic tests carried out on SAC-1 and SAC-2 specimens.

4.1. Static test

The block diagram of the static test setup is shown in Fig. 7. The free end of the specimen is subjected to loading using dead weight. The displacement of the composite beam is measured using a laser displacement sensor which senses the displacement based on the reflection of laser beam. The output of this sensor is connected to a computer to view the results. In static test the SAC specimen is clamped on one side and free end is loaded using dead weight of 1 N, as shown in Fig. 6. A Laser displacement sensor is used to measure the displacement of the SAC specimen during loading and unloading.
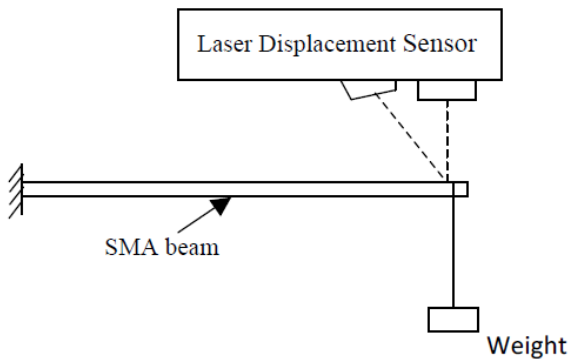

Fig. 7: Static test setup

Table 5: Results of the static test

Specimen type	Displacement in mm
SAC-1	17.1
SAC-2	4.14

4.2. Dynamic test

In dynamic test, the SAC specimen is clamped onto the vibration block as a cantilever beam. An instrumented impulse hammer is used as source of excitation. An accelerometer is mounted on the beam as shown in Fig. 8. A maximum frequency band of 512 Hz is selected for acquisition with resolution of 0.5 Hz. The frequency response function (FRF) plots thus obtained provide us the vibration characteristics such as frequency and mode shapes of the SAC specimen. The experimental frequencies obtained by the dynamic test, for SAC-1 and SAC-2 are tabulated in the Table 6. The FRF curves obtained from the test are shown in Fig. 9. It is observed that the two peaks in the plot represent the first two bending modes of the beam.
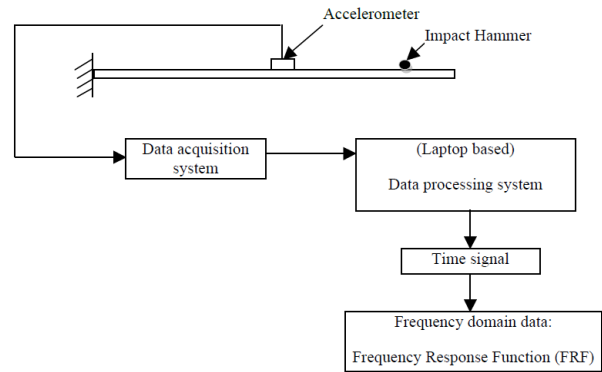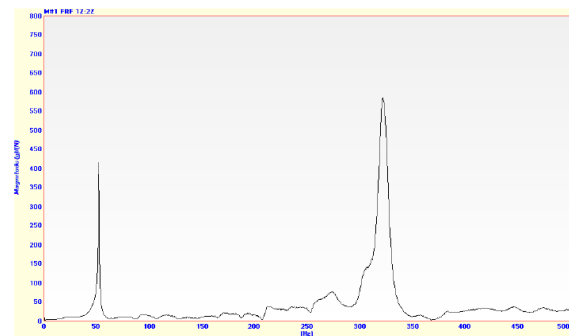

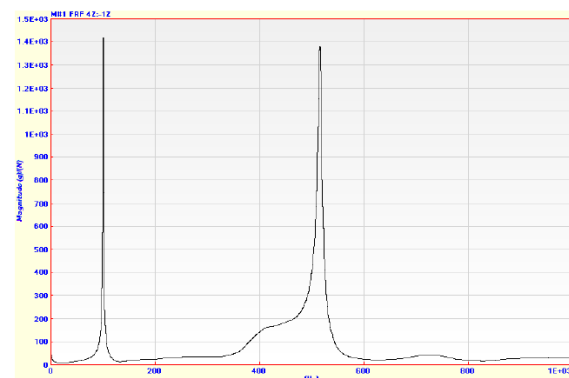**Fig. 8(a): Dynamic test setup block diagram**

Fig. 8(b): Dynamic test actual setup

Table 6: Experimental results of dynamic test

Mode No.	Frequency of SAC-1	Frequency of SAC-2	Mode description
1	51.8 Hz	101 Hz	First mode
2	322 Hz	507 Hz	Second mode

Fig. 9(a): FRF curves SAC-1

Fig. 9(b): FRF curves SAC-2

5. Results and discussion

Finite element analysis is conducted for the SAC specimens and the results thus obtained are verified by the experimental results. The measured tip displacements of both SAC specimens obtained by static experiment are compared with the tip deflections obtained through static FE analyses. Experimental modal tests were conducted on SAC-1 and SAC-2 specimens, and dynamic modal finite element analysis was also conducted. The frequencies for various models are obtained by both methods, however from dynamic test, only the frequencies for the first two modes could be obtained. The beam tip deflections obtained by static finite element analysis and experimental test are given in Table 7. We see that there is close agreement between the values for both SAC-1 and SAC-2, and the experimental value of tip displacement for SAC takes an upper hand over FEA value. While the difference between static experimental and FEA tip deflections for SAC-1 is 0.2 mm, for SAC-2 it is 0.48 mm.

Table 7: Beam tip deflections (static FEA and experimental)

	Tip deflection - FEA	Tip deflection - experimental
SAC-1	16.9 mm	17.1 mm
SAC-2	5.62 mm	5.14 mm

The frequencies of SAC-1 obtained by both modal FEA and experimental modal tests are presented in Table 8. We see that the frequencies are closely matching in both modes. It implies that the stiffness assumed is close to the specimen's actual stiffness. Similar frequencies of SAC-2 obtained by both modal FEA and experimental modal tests are presented in Table 9. We see that the frequency of first mode is closely matching. However the second mode shows significant deviation of nearly 120 Hz. The reason for this may the applied boundary condition. The increased clamping force would probably give better results. Since the first mode is matching assumed stiffness can be taken to be equal to the specimen's actual stiffness. The variation in second mode frequency is only because of the boundary condition.

Table 8: Dynamic FEA and experimental test results for SAC-1

Mode No.	Frequency - FEA	Frequency - experimental	Mode description
1	51.01 Hz	51.8 Hz	Bending - 01
2	319.16 Hz	322 Hz	Bending - 02

Table 9: Dynamic FEA and experimental test results for SAC-2

Mode No.	Frequency - FEA	Frequency - experimental	Mode description
1	100.30 Hz	101 Hz	Bending - 01
2	627.17 Hz	507 Hz	Bending - 02

6. Conclusions

In the presented work, the preparation, testing and analysis of smart adaptive composite beam have been successfully carried out. We understand that even though SMA there are ample benefits for the application of SMA as a smart component in fibre reinforced smart composites, there are yet many impediments to be addressed in the manufacture, long term application of these composite materials. In this research, the static and dynamic tests were carried out over a short duration, and hence the studies over larger operational times and for variable loading conditions shall be possibilities for extension of the research activity.

REFERENCES:

[1] T.W. Duerig, K.N. Melton, D. Stkel and C.M. Wayman. 1990. *Engineering Aspects of Shape-Memory Alloys*, Butterworth-Heinemann, Boston.

[2] V. Birman, K. Chandrashekhara and S. Sain. 1996. An approach to the optimization of shape memory alloy hybrid composite plates subject to low-velocity impact, *Composites, Part B*, 27, 439-446. https://doi.org/10.1016/1359-8368(96)00010-8.

[3] R. Stalmans, L. Delaey and J. Van Humbeeck. 1997. Modelling of adaptive composite materials with embedded shape memory alloy wires, *Mater. Res. Soc. Symp. Proc.*, 459, 119-130. https://doi.org/10.1557/PROC-459-119.

[4] S. Marfia, E. Sacco and J.N. Reddy. 2003. Superelastic and shape memory effects for laminated SMA beams, *AIAA J.*, 41(1), 100-109. https://doi.org/10.2514/2.1918.

[5] S. Marfia and E. Sacco. 2005. Micromechanics and homogenization of SMA-wire-reinforced materials, *J. Applied Mechanics*, 72(2), 259-268. https://doi.org/10.1115/1.1839186.

[6] M. Cherkaoui, Q.P. Sun and G.Q. Song. 2000. Micromechanics modelling of composite with ductile matrix and shape memory alloy reinforcement, *Int. J. Solids Struct*, 37, 1577-1594. https://doi.org/10.1016/S0020-7683(98)00332-1.

[7] C.S. Jarali and S. Raja. 2008. Homogenization and pseudoelastic behaviour of composite materials reinforced with shape memory alloy fibres, *J. Composite Materials*, 42, 1685-1707. https://doi.org/10.1177/0021998308092201.

[8] C.S. Jarali, S. Raja and A.R. Upadhya. 2008. Micro-mechanical behaviours of SMA composite materials under hydro-thermo-elastic strain fields, *Int. J. Solids and Structures,* 45, 2399-2419. https://doi.org/10.1016/j.ijsolstr.2007.12.003.

[9] H.J. Lee, J.J. Lee and J.S. Huh. 1999. A simulation study on the thermal buckling behaviour of laminated composite shells with embedded shape memory alloy wires, *Compos. Struct.*, 47, 463-469. https://doi.org/10.1016/S0263-8223(00)00020-9.

[10] B. Noolvi, S. Raja, S. Nagaraj and V.R. Mudradi. 2017. Fabrication and testing of SMA composite beam with shape control, *AIP Conference Proc.*, 020055. https://doi.org/10.1063/1.4990208.